

The Pure Nuclear Electric Quadrupole Resonance of N^{14} in Three Molecular Solids*

G. D. WATKINS AND R. V. POUND
Harvard University, Cambridge, Massachusetts
(Received January 28, 1952)

By using an rf spectrometer¹ of the regenerative type, the pure quadrupole resonance of N^{14} has been observed in three solids: cyanogen iodide, cyanogen bromide, and hexamethylene-tetramine. An "on-off" square wave of magnetic field at 280 cps was applied to the sample. In this way, the resonance was smeared out for half of the modulation period and 280 cps modulation of the absorption resulted. A narrow band amplifier, a phase sensitive detector, and an integrating output circuit were used and the signal was displayed on a recording meter. Figure 1 shows the recorded signal in $(CH_2)_6N_4$ at room temperature. The amplitude ratio of signal-to-noise in BrCN and ICN is only about one-tenth as large as this, as a result mainly, of longer relaxation times and lower density of nitrogen. A ten-times longer integration time constant was used in observing these lines to compensate partially for the loss in signal intensity. Defining the width of an absorption as $[g_{\max}(\nu)]^{-1}$, where $g(\nu)$ is the normalized shape function of the line, the observed widths are 1.05 kcps, 760 cps, and 1.08 kcps for ICN, BrCN, and $(CH_2)_6N_4$, respectively.

The frequencies were measured at room, ice, dry ice, and liquid N_2 temperatures and these data are given in Table I.

TABLE I. Frequency (Mcps) vs temperature.

Temperature	$(CH_2)_6N_4$	BrC≡N	IC≡N
-196°C	3.4076 ± 0.0001	(1) 2.5109 ± 0.0001 (2) 2.5203 ± 0.0001	—
- 74°C	3.3560 ± 0.0001	(1) 2.4910 ± 0.0002 (2) 2.4963 ± 0.0002	2.5512 ± 0.0002
0°C	3.31990 ± 0.00005	2.4734 ± 0.0002	2.5451 ± 0.0002
Room temp.	3.3062 ± 0.0001 (26.6°C)	(1) 2.4650 ± 0.0002 (2) 2.4627 ± 0.0002 (24.2°C)	2.5424 ± 0.0002 (26.8°C)

A search over the range 2.52–2.57 Mcps failed to detect the absorption in ICN at liquid N_2 temperature. While warming up from this temperature, the crystal grains appeared to fracture violently just below dry ice temperature, possibly evidence of a

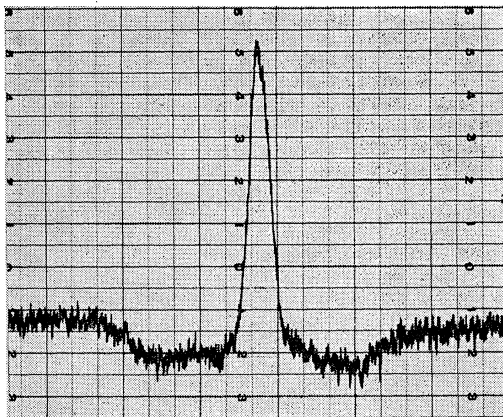


FIG. 1. Pure quadrupole absorption of N^{14} in $(CH_2)_6N_4$. The negative deflections in the wings correspond to the absorption when the modulating magnetic field is on. Each of the two cascaded RC integrating circuits has a time constant of 2 sec.

phase change, and associated strains may have so broadened the line that it was undetectable. In BrCN, two lines of approximately equal intensity were observed. They have different temperature dependences and cross at 0°C. This could result if there were two nonequivalent molecules per unit cell or if there were a temperature dependent asymmetry factor $\eta = [(\partial^2 V / \partial x^2) - (\partial^2 V / \partial y^2)] / (\partial^2 V / \partial z^2)$. For $I=1$, departure from axial symmetry would remove the $m_I = \pm 1$ degeneracy and two lines would result. No data on crystal structure for BrCN has been found in the literature. Neither of the above sources of doubling of the N^{14} resonance would be present if the unit cell were similar to the unimolecular rhombohedral cell of ICN.² Information on this point could be obtained by observation of the Zeeman pattern in a single crystal.³ In the gas state, quadrupole coupling constants e^2qQ/h of 3.83 ± 0.08 and 3.80 Mcps are reported for BrCN⁴ and ICN⁵, respectively. For $I=1$, the resonance is at $\nu = \frac{3}{2}e^2qQ/h$ and the coupling constants are thus about 12 percent smaller in the solid than in the gaseous state.

Relaxation times were measured by the saturation method and for ICN, BrCN, and $(CH_2)_6N_4$ they are, at 0°C, 7.4 sec, 2.7 sec, and 0.17 sec, respectively. For samples of the size used (2.5 cm^3) and these relaxation times, the rf voltages at the coil for optimum signal-to-noise are 0.19 v(rms), 0.26 v(rms), and 1.6 v(rms), respectively. At these levels, the noise figure of the spectrometer is low,¹ and little could be gained by the use of more complicated detection systems.

The relaxation time in $(CH_2)_6N_4$ was found to be 1.7 sec at -74°C and 11 sec at -196°C . If we assume the model of Bayer,⁶ in which the relaxation mechanism arises from the torsional oscillations of the molecule as a whole, a dependence $T_1 \sim \tau_a T^{-1}$ is predicted, where τ_a is the average lifetime of the various states of torsional oscillation. This is not compatible with the rapid temperature dependence of T_1 that is observed unless τ_a varies with temperature.

* This work was partially supported by the joint program of the ONR and AEC.

¹ G. D. Watkins and R. V. Pound, Phys. Rev. **82**, 343 (1951).

² R. W. G. Wyckoff, *Crystal Structures I* (Interscience Publishers, Inc., New York, 1948).

³ C. Dean, Bull. Am. Phys. Soc. **27**, No. 1, 32 (1952).

⁴ Townes, Holden, and Merrit, Phys. Rev. **74**, 1113 (1948).

⁵ Smith, Ring, Smith, and Gordy, Phys. Rev. **73**, 633 (1948).

⁶ H. Bayer, Z. Physik **130**, 227 (1951).

The Photodissociation of the Deuteron by High Energy Gamma-Rays

SEISHI KIKUCHI

Radiation Laboratory, Department of Physics, University of California, Berkeley, California
(Received January 23, 1952)

AN analysis was made of proton tracks found in photographic emulsions exposed to the secondary particles from a high pressure deuterium gas target bombarded by the synchrotron bremsstrahlung gamma-rays of maximum energy 320 Mev,¹ with the object of investigating the photodissociation of the deuteron in the high energy region. The secondary particles were collimated by slit systems in such a manner that we could analyze the protons at emission angles of approximately 45, 90, and 135 degrees.

The minimum energy required for a proton to penetrate through the walls of the target chamber to reach the plates was 70 Mev at 45 and 135 degrees and 60 Mev at 90 degrees. This circumstance excluded the possibility of recoil protons ejected by the photo-meson producing process from reaching the plates. The energy of the proton was computed from the thickness of the absorbing material between the end point of the proton and the target.

In the case of the photo-dissociation of a deuteron into a proton and a neutron, there is a relation $k = 2T[1 - (T/M)(P \cos \theta/M)]^{-1}$ between the energy T and momentum P of the proton of mass M ,

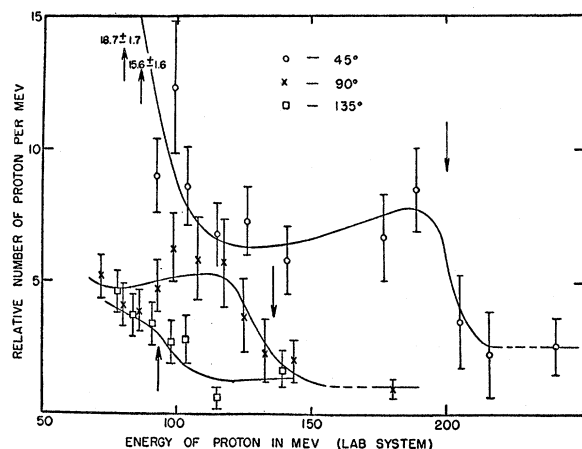


FIG. 1. Differential cross section per photon for the photodissociation, as a function of the photon energy.

the angle θ between the direction of the ejection and the incident beam, and the energy k of the photon which caused the dissociation.

Putting $k=320$ Mev in this relation we get 93, 136, and 200 Mev for the maximum energy of protons at 45, 90, and 135 degrees, respectively.

The energy spectra obtained are shown in Fig. 1. These spectra show well defined cutoffs at the proton energies 95, 135, and 200 Mev, coinciding closely with the expected values. This seems to indicate that these protons are actually the photoprotons produced by the splitting of a deuteron into a proton and a neutron by the absorption of a photon.

Assuming the bremsstrahlung spectrum to be proportional to $1/E$, we can compute from the results shown in Fig. 1, the differential cross section per photon for the photodissociation as a function of the photon energy. The result is given in Table I.² In

TABLE I. Differential cross section as a function of photon energy in the laboratory system.

Energy of photon in Mev	Diff. cross sec in microbarns	Energy of photon in Mev	Diff. cross sec in microbarns
133	14.4 ± 1.8	158	2.7 ± 0.6
144	12.8 ± 1.9	178	2.4 ± 0.7
152	6.6 ± 1.8	194	2.4 ± 0.7
162	10.7 ± 3.0	211	3.4 ± 1.0
170	6.9 ± 2.2	226	5.1 ± 1.3
189	5.4 ± 2.1	248	5.2 ± 1.7
205	6.5 ± 2.3	272	5.5 ± 1.3
228	5.0 ± 2.6		
285	8.0 ± 3.8	135° { 250	0.99 ± 0.27
304	12.3 ± 4.0	272	0.99 ± 0.35

the 45-degree case one can see the dependence of the cross section on photon energy in a fairly wide range. Below 150 Mev it decreases rather steeply with increasing energy, and at about 150 Mev it begins to flatten out and then starts to increase again with increasing energy.

The angular distribution in laboratory system shows a fairly strong forward asymmetry. The same trend can be seen in the center-of-mass system.

The total cross section was roughly estimated by multiplying the differential cross section at 90° by 4 π . Below 150 Mev, where no data for 90° was available, the cross section was assumed to be proportional to the differential cross section at 45°. Table II shows the results. The errors indicated are those referred to the relative values. Referring to the absolute value, the error might be as large as a factor of 3. Comparing with Schiff's theoretical values given in Table II, one should rather consider that the

TABLE II. Total cross section as a function of photon energy.

Energy of photon in lab. system	Energy of photon in c.m. system	Total cross section in 10 ⁻²⁹ cm ²	Theoretical value (Schiff), in 10 ⁻²⁹ cm ²
133	125	6.2 ± 0.5	2.3
158	146	3.4 ± 0.8	1.6
178	163	3.0 ± 0.8	
194	176	3.0 ± 0.9	
211	191	4.3 ± 1.2	
226	202	6.4 ± 1.7	
248	220	6.6 ± 2.2	
272	239	6.9 ± 1.7	

experimental values are compatible with the theoretical values below 150 Mev, which is the upper limit of the validity of the theory set by Schiff himself. Above 150 Mev the cross section does not decrease as the straightforward extrapolation of Schiff's curve does. Recently, Gilbert and Rose³ at this Laboratory studied the photodissociation of the deuteron in nearly the same energy range as the present work, using a counter technique. For the dissociation at photon energies of 200 and 250 Mev in the c.m. system, they obtained total cross sections which are about twice as large as the present values. Because of the relatively large error involved in both experiments, the results should be regarded as in agreement with each other.

The increase of the photodissociation cross section above 150 Mev may be explained by the increasing importance of the absorption of a photon with emission and reabsorption of a virtual meson in the energy range above the meson threshold. It is hoped that the experimental evidence given here may provide a more direct and more stringent test for the different types of meson theory, than has been the case with experiments in the low energy region, where the comparison of the theory with the experiments was made more or less indirectly, as far as the meson theory is concerned.

The author wishes to thank Professors McMillan and Helmholtz, and R. S. White and W. S. Gilbert for discussions as well as for their generosity in placing their plates at the author's disposal.

¹ The exposure had been made originally by R. S. White and others of this laboratory to investigate the photomeson production in deuterium [Bull. Am. Phys. Soc. 26, No. 8, 22 (1951)].

² The relatively large error in the 45° case compared to the other cases came from the ambiguity involved in the background.

³ W. S. Gilbert and J. W. Rose, Phys. Rev. (to be published).

Silver-Activated Alkali Halides

H. W. ETZEL, J. H. SCHULMAN, R. J. GINTHER, AND E. W. CLAFFY
Crystal Branch, Metallurgy Division, Naval Research Laboratory,
Washington, D. C.

(Received February 4, 1952)

THE earliest investigation of the silver-activated alkali halides appears to have been made by Smakula.¹ His data show a single sharp absorption band peaking at 2100Å in NaCl:Ag. The most recent study of these phosphors is evidently by Kato,² who investigated the emission as well as the absorption spectra. Kato's absorption data agree very well with Smakula's. He observes that excitation into the characteristic silver ion absorption band in NaCl:Ag produces two emission bands, one peaking at 2490Å and a second at 4000Å.

We have found, as shown in Fig. 1, that three absorption bands appear in NaCl upon the introduction of ionic silver. These bands lie at 2095Å, 2170Å, and 2295Å. The absorption measurements were made with a split-beam, frequency selective, single detector, automatic recording spectrophotometer³ on single crystals grown by the Kyropoulos technique from NaCl-AgCl melts. Figure 2 is a photograph of the emission of the NaCl:Ag upon excitation into each of the three absorption bands. For this measurement